



Synthesis and characterization of PbS nanowires doped with Tb³⁺ ions by using chemical bath deposition method

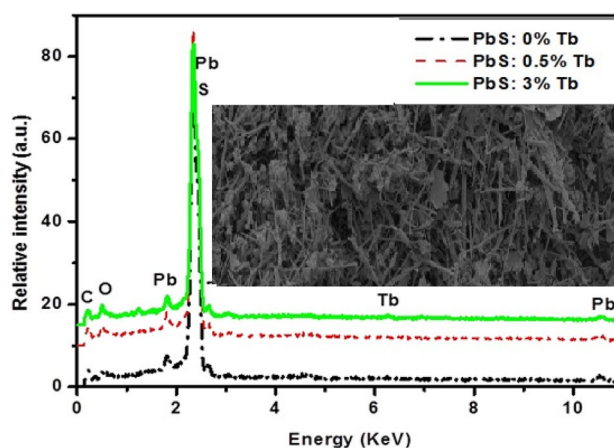
L. F. Koao¹ · Fekadu Gashaw Hone^{1,2} · F. B. Dejene¹

Received: 3 September 2019 / Accepted: 6 December 2019 / Published online: 17 December 2019
© The Author(s) 2019

Abstract

Crystalline lead sulfide (PbS) nanowires doped with terbium (Tb³⁺) ions were synthesized by the chemical bath deposition method at room temperature. The powder was obtained from an aqueous solutions using lead acetate dehydrate, terbium nitrate, thiourea, potassium hydroxide and ammonia. The terbium molar concentrations were varied in the deposition process to investigate the effect on the structural, optical, morphological and luminescent properties of PbS nanowires. The crystalline size was found to be dependent on the concentration of the Tb³⁺ ions used. The estimated average crystalline sizes were calculated from the X-ray diffraction and found to be 34, 33 and 37 nm for PbS: 0% Tb³⁺, PbS: 0.2% Tb³⁺ and PbS: 0.5% Tb³⁺, respectively. The scanning electron microscopy micrographs depict nanowire shape for the undoped as well as Tb-doped samples. The energy-dispersive X-ray and Auger electron spectroscopy analyses confirmed the presence of all the expected elements. The solid powder nanowires exhibited high absorptions in the UV–Vis regions. The band gap energies were estimated in the range of 1.99–2.46 eV. The absorption edge and the band gap energies of these PbS nanowires have shifted depending on the concentration of the dopant. The maximum luminescence intensity was obtained for PbS: 0.2% Tb³⁺ ions and luminescent quenching was observed for higher terbium concentrations.

Graphic abstract



Keywords Lead sulfide · Doping · CBD method · Nanowires · Nanopowder

✉ Fekadu Gashaw Hone
fekeye@gmail.com

¹ Department of Physics, University of the Free State (Qwa Qwa Campus), Private Bag X13, Phuthaditjhaba 9866, South Africa

² Department of Physics, Addis Ababa University, P.O. Box 1176, Addis Ababa, Ethiopia

Introduction

Solution chemistry has been applied to many mixed sulfide and oxide systems for preparation of semiconductors, photocatalysts, glasses, coatings, and other materials [1].



Nowadays, nanomaterials have several functionalities and enhanced physical and chemical properties [2]. Among them, one-dimensional semiconductor phosphor nanocrystal structures have been extensively studied for the last two decades because of their unusual structural, electronic, and optical properties [3]. Lead sulfide (PbS) is among the IV–VI group semiconducting material with direct band gap of 0.41 eV at room temperature and a space group of $Fm\bar{3}m$ [4]. Moreover, its absorption coefficient continuously increases from the infrared to the visible region [5]. PbS nanowires are potentially useful in electroluminescent devices such as light-emitting diodes, lasers, solar cells and biological systems [6, 7] bioimaging [8]. PbS nanowires can be easily incorporated into polymer, glassy matrices where they can be applicable in fiber-optics telecommunication [9] and again can be incorporated in semiconductor nanoparticles (e.g., ZnO and ZnS) where they can be applied in light-emitting diodes, laser diodes and ultraviolet photodetectors [9]. The band gap energy of PbS can be changed from 0.41 eV to the values up to 5.2 eV by varying the shape and size from the bulk materials to nanocrystal structures [10]. Several synthesis techniques such as microemulsion [11], chemical bath deposition (CBD) [12], sol–gel [13], solvothermal process [14] and sonochemical method [15] have been used to synthesize undoped PbS nanocrystal structures. The PbS nanoparticles embedded in an amorphous silica (SiO_2) host were also investigated [16]. Doping with optically active luminescent materials controls the band structure of the nanocrystal structures and shows intense emissions in a wide range of wavelength depending on the impurity type, concentration and crystal dimensions and also play key roles in luminescence efficiency. Doping with rare earth ions (RE^{3+}) influences the band structure, surface morphology and crystalline size of the nanomaterials. Among the RE^{3+} ions, Tb^{3+} is one of the popular efficient luminescent materials. Particularly, Tb^{3+} could be used as phosphorous for fluorescent lamps and emission agents, or sensitizing agents for plasma displays [17]. Literature review showed that many doping metal atoms have been used to improve the chemical and physical properties of PbS nanowires; however, no study is available so far on the synthesis and characterization of PbS nanowires doped with Tb^{3+} ions. The main objective of this report is to provide a comprehensive study on the effects of Tb^{3+} doping on the structural, optical, morphological and the photoluminescence properties of PbS nanowires using cost-effective and eco-friendly chemical bath deposition route. The chemical bath deposition is simple, inexpensive and works at low temperatures [18]. The study of the effects of Tb^{3+} concentration on the photoluminescence nature of PbS one-dimensional nanostructures is very limited and will remain a subject of great interest. In the present

study, we also report for the first time the synthesis and characterization of PbS nanowires doped with lanthanides group Tb^{3+} ions.

Experimental details

Synthesis of the nanopowder

All the chemicals used for the preparation of the nanopowders were of analytical grade. It includes lead acetate dehydrate ($\text{Pb}(\text{CH}_3\text{COO})_2 \cdot 2\text{H}_2\text{O}$), terbium (iii) nitrate hexahydrate ($\text{Tb}(\text{NO}_3)_3 \cdot 6\text{H}_2\text{O}$), thiourea ($(\text{NH}_2)_2\text{CS}$), potassium hydroxide (KOH) and ammonia (NH_3). All the solutions were prepared using deionized water. During the preparation of the nanopowders, ammonia was used as a complexing agent, potassium hydroxide was applied to adjust the pH of the chemical bath and thiourea was used as the source of the sulfide ions. The preparations of undoped PbS nanostructures were carried out using the following procedure: 65 ml of lead acetate dehydrate (0.45 M) solutions was added in to a 200-ml beaker; then, 65 ml of thiourea (0.15 M) solution was added into the same reaction beaker and the mixture was stirred for a few seconds; at this stage, the solution was very clean. Next, 50 ml of ammonia (28%) solution was added slowly into the mixture then the solution left for 2 hrs at room temperature to stir continuously. The terbium-doped PbS nanostructures were prepared by changing the different molar concentrations of terbium nitrate and holding the amount of lead acetate dehydrate, thiourea and ammonia constant. To prepare Tb-doped PbS nanowires, terbium nitrate hexahydrate (9.812×10^{-2} M) with different concentrations 0, 0.2, 0.5 and 3 at.% was used by changing the molar ratio of lead acetate dehydrate and terbium nitrate hexahydrate. All the samples were synthesized at room temperature at a pH of 10.56. The formed precipitates were filtered and washed with ethanol several times. The resulting powders were dried at ambient conditions for 3 days and ready for characterization.

Characterization

The crystal structures of the samples were determined using a Bruker AXS Discover diffractometer with $\text{CuK}\alpha$ (1.5418 Å) radiation. The morphology of the prepared nanoparticles was investigated by scanning electron microscopy (SEM) using a Shimadzu model ZU SSX-550 Superscan coupled with an energy-dispersive X-ray spectrometer (EDX). Auger electron spectroscopy (AES) was performed in a PHI 700 Scanning Auger Nanoprobe. The reflectance measurements were carried out in the range of 200–800 nm wavelength using a Perkin Elmer UV/Vis Lambda 20 Spectrophotometer. The Photoluminescence (PL) measurements

were done on a Carry Eclipse Fluorescence Spectrophotometer system, equipped with a 150-W xenon lamp as the excitation source. All the samples used were in the powder form.

Results and discussions

Structural, morphological and compositional analyses

The X-ray diffraction (XRD) patterns of the Tb-doped and undoped PbS nanowires are displayed in Fig. 1. The diffraction pattern of undoped PbS nanowires confirmed that the prepared samples were well matched with the standard JCPDS data file reference code: 05-0592 (Galena).

The four main peaks observed in the diffractogram (Fig. 1) around 25.99° , 30.11° , 43.09° and 51.03° could be assigned to the planes (111), (200), (220) and (311), (422) of the FCC crystal structure. From the figure, it was also observed that at lower Tb concentration, there is no noticeable effects on the diffraction patterns; however, as Tb concentration was increased, additional peaks were immersed and they may be attributed to unreacted $\text{Pb}(\text{CH}_3\text{COO})_2 \cdot 2\text{H}_2\text{O}$ precursor (confirmed by JCPDS card No. 18-1738). From the XRD diffractogram, it was also observed that there is a slight peak shifts towards the higher 2θ values as Tb^{3+} ions incorporated into PbS nanopowder. Since the ionic radius of Tb^{3+} ion (0.923 \AA) is smaller than that of Pb^{2+} (1.19 \AA), incorporation of terbium ions into the Pb^{2+} position is expected to shift the diffraction peaks to higher 2θ values. This shift in the diffraction peaks of $\text{PbS}:\text{Tb}^{3+}$ nanopowder strongly confirmed the successful incorporations of terbium ions into PbS lattice. The experimental values of the lattice constants were 5.9504 \AA for undoped PbS and PbS doped

with 0.2% of Tb, 5.9413 \AA and 5.7895 \AA for PbS: 0.5% Tb and PbS: 3% Tb, respectively. These results confirmed that the lattice parameter decreased slightly with an increasing of the mol concentration of Tb^{3+} . The average crystalline size of the as-prepared nanocrystals was calculated from the full width at half maximum (FWHM) of the diffraction peaks using the Debye–Scherrer formula [19]. All major diffraction peaks were chosen to estimate the average size of the nanocrystals by the least square method. The estimated crystalline sizes were 34, 33 and 37 nm for undoped PbS, PbS: 0.2% Tb and PbS: 0.5% Tb, respectively. It is clear that the average crystalline size increased slightly as the molar concentration of Tb^{3+} ions increased.

Figure 2a, b shows the representative SEM micrographs of the undoped and Tb-doped PbS nanowires. The surface aspects of all the SEM images are composed of nanowires. It is clear that all the nanowires are clustered and not homogeneous. The morphology of the products is not affected by the precursor concentration in the solution.

From Fig. 3, the EDX elemental analyses of the nanowires suggest the presence of Pb and O (from the cores and the outside shell) and C (from the C double sided tape) and a small shoulder to the right of the Pb peak due to overlapping of the S and Pb peaks. At the low molar percentages of the dopant (PbS: 0.2% Tb^{3+}), there is no visible peak of Tb^{3+} , probably due to their relatively low concentration in the PbS matrix, and at the high molar concentration of the dopant (PbS: 3% Tb^{3+}), a peak of Tb^{3+} ions is detected. Due to the overlapping between the Pb and the S signal in the EDX spectra, AES measurements were carried out to double check the elements and to evaluate their purity. The Auger spectrum of the undoped PbS nanowires is shown in Fig. 4. The typical spectrum of the nanowires confirms the presence of Pb and S. The signals at binding energies of 517 eV and 276 eV are ascribed to the presence of adventitious oxygen and carbon, respectively, which come from the adsorbed gases molecules in the ultra-high vacuum (UHV) chamber rather than evidence for the deposition of oxide material. The presence of N may be attributed to impurity due to the ambient conditions. Moreover, no other impurities were found on the surface of the PbS nanowires, suggesting that the as-synthesized PbS nanowires are relatively pure.

Optical properties

Figure 5 shows the typical variations of the optical absorption spectra of the undoped and Tb-doped powders samples. Both the undoped and 0.2% Tb-doped PbS samples display two major absorption bands at 431 and 601 nm. At high doping concentration of the Tb^{3+} ions (0.5%), the absorption band at low wavelength shifts from 431 to 408 nm. This may be due to the peaks of lead acetate that

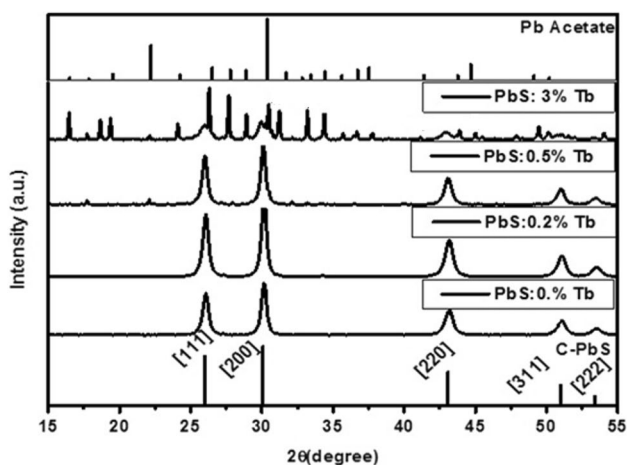


Fig. 1 The XRD diffraction patterns for undoped and Tb-doped PbS nanopowders



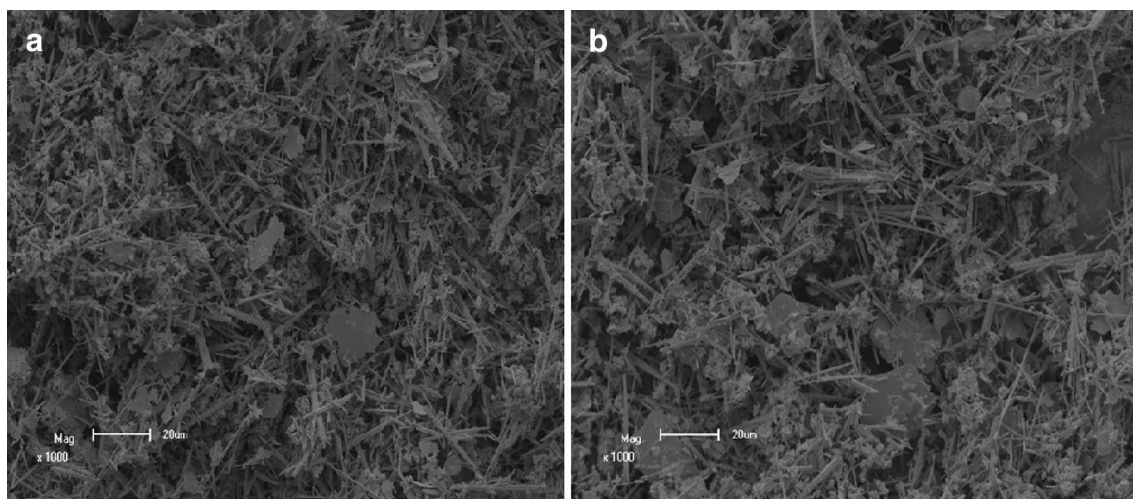


Fig. 2 The SEM images of **a** pure PbS and **b** PbS: 3% Tb nanowires

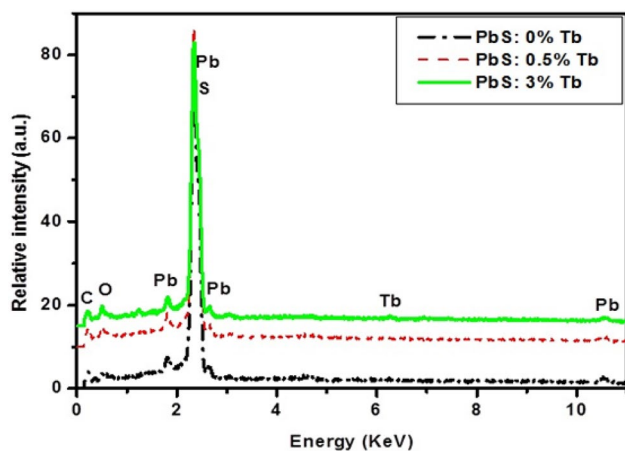


Fig. 3 A representative EDX spectrum of the undoped and Tb-doped PbS nanowires

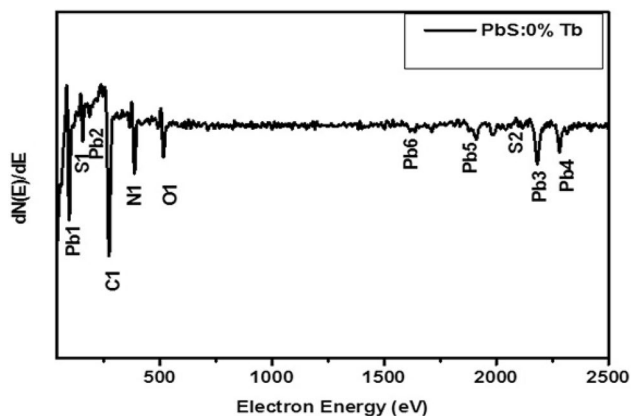


Fig. 4 Auger spectra of the undoped PbS nanowires

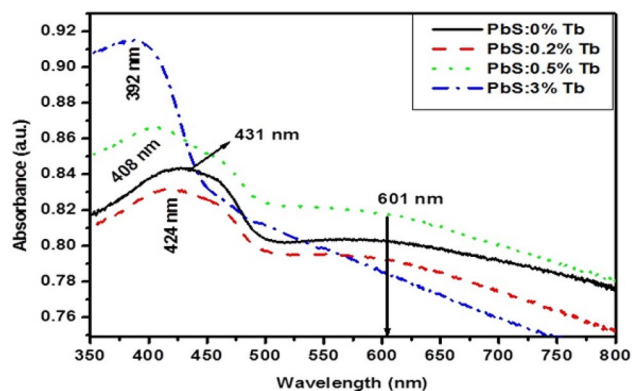


Fig. 5 The absorbance spectra of undoped and Tb-doped PbS nanowires

are starting to emerge at Tb (0.5%)-doped PbS nanowires as confirmed by the XRD results.

At high molar concentrations of 3% of Tb^{3+} , the UV–Visible spectrum shows one broad absorption band around 392 nm. It is clear from the absorption spectra that the broad absorption for PbS around 601 nm was quenched as the molar concentration of Tb^{3+} ions increased. The absorption bands at around 392 nm may be due to the presence of lead acetate, which confirms the appearance of the diffraction peaks of these impurities in the XRD spectra as the Tb ions increased. Lastly, the absorption intensity increased as the molar concentration of Tb^{3+} ions increased especially in the UV region. This increase in absorption intensity might be due to the increase in crystalline sizes as the molar concentration of Tb^{3+} increased. The energy band gap of these materials was estimated using the following equation [20].

$$\alpha hv = (hv - E_g)^n, \quad (1)$$

where α absorption coefficient, hv is the photon energy, E_g is the band gap $n=2$ for direct transitions. The energy band gaps were measured with the help of absorption spectra plotting graphs of $(\alpha hv)^2$ versus hv , and the corresponding band gaps obtained from the extrapolating straight portion of the graph on the hv axis at $\alpha=0$. The estimated band gap energies of PbS: 0%Tb, PbS: 0.2%Tb, PbS: 0.5% Tb and PbS: 3% Tb were 2.46, 2.47, 2.32 and 1.99 eV, respectively (see Fig. 6). The plot of the PbS nanowires doped with 0.2% of Tb is not included to make the figure more clear. From the results, it is clearly noticed that the optical band gap energy of the doped PbS nanowires decreased as the concentrations of Tb^{3+} increased.

This result is in accordance with the crystalline size which are increased as the molar concentration of Tb^{3+} ions

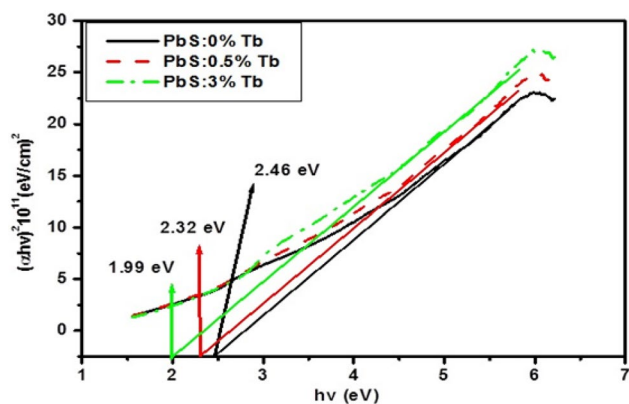


Fig. 6 The plot to determine the band gap energies of undoped and Tb-doped PbS nanowires

increased as confirmed by XRD analyses. The errors for the band gap energies of PbS: 0%Tb, PbS: 0.2%Tb, PbS: 0.5% Tb and PbS: 3% Tb were 0.04, 0.02, 0.03 and 0.02 eV, respectively, with an average of 0.03 eV.

Photoluminescence (PL)

The PL spectra of the samples when excited with a 330-nm wavelength are shown in Fig. 7a, b. The emission spectra depict a strong broad peak at around 425 nm and a less intense broad peak at around 720 nm. The PL peak at around 425 nm is associated with surface defects involving the transition of electrons from the conduction band edge to holes, trapped at interstitial Pb^{2+} sites [21]. It was observed that the presence of Tb^{3+} ions slightly affects the luminescence intensity in the IR region and not the luminescence wavelength. This emission at around 723 nm is due to the PbS nanostructures and may be due to band edge luminescence. The effects of Tb^{3+} ions concentrations on the maximum peak intensities of the blue emissions are clearly observed in Fig. 8. An increase in Tb^{3+} concentrations up to 0.2% Tb^{3+} ions increases the luminescence intensity (see Fig. 7). This may be due to the different valences between Tb^{3+} and Pb^{2+} which produced defects, because of charge compensation requirements, resulting in change of energy transfer with the presence of the Tb^{3+} ions. The excitation source was absorbed by Tb^{3+} ions (donor) and transferred non-radiatively to the PbS nanowires (acceptor). This implies that there is a possibility of dopant (Tb^{3+}) transferring energy to the host (PbS) just like ZnO– SiO_2 :Ce, in which ZnO transfers energy to SiO_2 :Ce [22].

A further increase in the Tb^{3+} ions above 0.2% resulted in luminescence quenching caused by non-radiative interaction between ions as the resonant energy transfer became

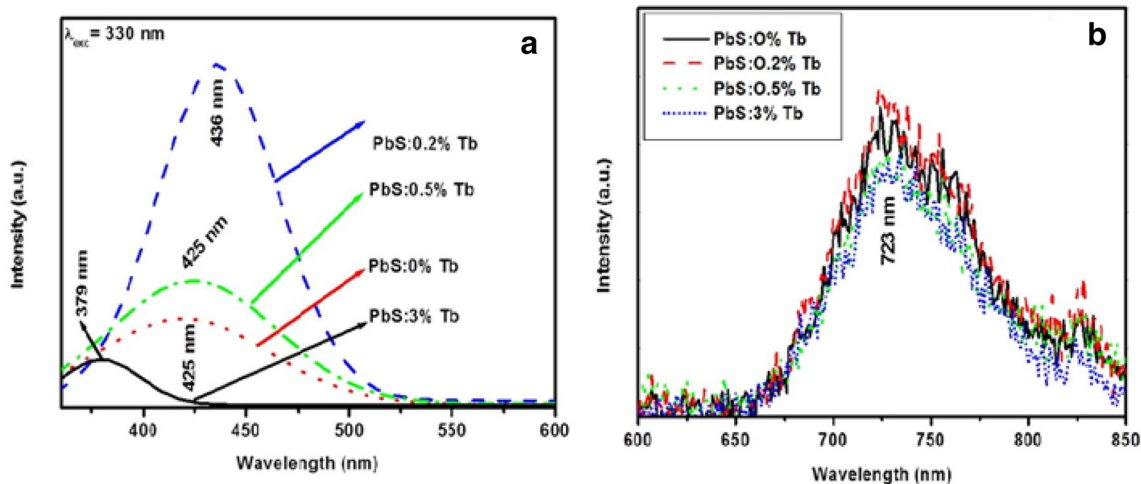


Fig. 7 The photoluminescence patterns for undoped and Tb-doped PbS nanowires showing intense **a** blue band emissions in the UV–Visible region and **b** emission in IR region



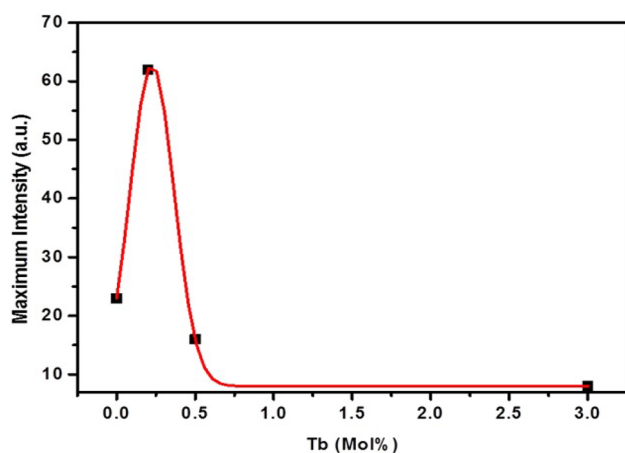


Fig. 8 The PL intensity of PbS nanowires as a function of Tb (mol%) concentrations

stronger. The terbium like other rare earths, at higher molar concentrations, has a low solubility in the PbS nanowires; therefore, Tb^{3+} ions tend to migrate to the PbS surface. Secondly, this decrease in luminescence intensity can be due to slightly increasing crystalline size as the molar concentration of Tb increased as confirmed by the estimated crystalline size from the XRD diffractogram analyses. Therefore, it is well understood that the non-radiative recombinations increase with increasing crystalline size and as a result, the luminescence intensity decreased [23, 24]. The positions of the emission peaks slightly shift from 425 to 436 nm; this shift is observed by increasing the Tb^{3+} content in PbS nanowires. This shift may be due to emerging lead acetate as confirmed by the XRD results. The position of the emission peak around 425 nm in the emission spectra shifted to the UV region around 379 nm for the 3% Tb sample. This shift is in correspondence with the shift from UV results and may be due to the presence of lead acetate, which confirms the appearance of the diffraction peaks of this impurity in the XRD diffractogram as the Tb ions increased.

Conclusion

The undoped and Tb-doped PbS nanowires have been successfully synthesized by the chemical bath deposition technique. The XRD results showed that the structure of the obtained material was face-centered cubic. It was also found that the estimated crystalline size from the XRD spectra increased as the molar concentration of Tb^{3+} ions increased. The SEM study verified that doping did not bring appreciable change on the morphology properties of PbS:Tb nanowires. The EDX and auger electron spectroscopy analyses have revealed the presence of Pb, S and Tb elements in the prepared nanowires. The UV–Vis study showed that the

absorption wavelength of the doped PbS nanowires shifts to the lower wavelength as the molar concentrations of Tb increased. It was also noticed that the band gap energy of PbS nanowires decreased with an increase of the molar concentrations of Tb^{3+} ions. At a Tb^{3+} concentration of 0.2 mol%, the PL intensity was found to be maximum. It was also observed that there was a shift of the luminescence wavelength from the visible region to the UV region as the molar concentrations of the dopant (Tb^{3+}) increased. This shift may be due to Tb promoting the impurities. The present results, therefore, should be a very significant step toward a convenient, economical and eco-friendly fabrication of PbS:Tb nanowires for various applications.

Acknowledgements The author would like to acknowledge the National Research Foundation and Department of Science and Technology and the University of the Free State for financial support.

Open Access This article is licensed under a Creative Commons Attribution 4.0 International License, which permits use, sharing, adaptation, distribution and reproduction in any medium or format, as long as you give appropriate credit to the original author(s) and the source, provide a link to the Creative Commons licence, and indicate if changes were made. The images or other third party material in this article are included in the article's Creative Commons licence, unless indicated otherwise in a credit line to the material. If material is not included in the article's Creative Commons licence and your intended use is not permitted by statutory regulation or exceeds the permitted use, you will need to obtain permission directly from the copyright holder. To view a copy of this licence, visit <http://creativecommons.org/licenses/by/4.0/>.

References

1. Khanmohammadi, M., Fard, H.G., Garmarudi, A.B., Khoddami, N.: Fourier transform infrared spectroscopic monitoring of sol-gel process in synthesis of PbS–TiO₂ hybrid nanostructures. *Thin Solid Films* **518**, 6729–6732 (2010)
2. Bashir, B., Warsi, M.F., Khan, M.A., Akhtar, M.N., Gilani, Z.A., Shakir, I., Wadood, A.: Rare earth Tb^{3+} doped LaFeO₃ nanoparticles: new materials for high frequency devices fabrication. *Ceram. Int.* **41**, 9199–9202 (2015)
3. Acharya, S., Gautam, U.K., Sasaki, T., Bando, Y., Golan, Y., Ariga, K.: Ultra narrow PbS nanorods with intense fluorescence. *J. Am. Chem. Soc.* **130**, 4594–4595 (2008)
4. Hone, F.G., Dejene, F.B., Echendu, O.K.: Band gap tailoring of chemically synthesized lead sulfide thin films by in situ Sn doping. *Surf. Interface Anal.* **50**, 648–656 (2018)
5. Pawar, S.B., Shaikh, J.S., Devan, R.S., Ma, Y.R., Haranath, D., Bhosale, P.N., Patil, P.S.: Facile and low cost chemosynthesis of nanostructured PbS with tunable optical properties. *Appl. Surf. Sci.* **258**, 1869–1875 (2011)
6. Preetha, K.C., Remadevi, T.L.: Behavior of chemically deposited PbS thin films subjected to two different routes of post deposition annealing. *Mater. Sci. Semicond. Process* **16**, 605–611 (2013)
7. Wan, Q., Huang, Q., Liu, M., Xu, D., Huang, H., Zhang, X.: Wei Y (2017) Aggregation-induced emission active luminescent polymeric nanoparticles: non-covalent fabrication methodologies and biomedical applications. *Appl. Mater. Today* **9**, 145–160 (2017)



8. Jiang, R., Liu, M., Chen, T., Huang, H., Tian, J., Wen, Y., Cao, Q., Zhang, X., Huang, Q., Wei, Y., Choubey, A.: Facile construction and biological imaging of cross-linked fluorescent organic nanoparticles with aggregation-induced emission feature through a catalyst-free azide-alkyne click reaction. *Dyes Pigments* **148**, 52–60 (2018)
9. Ntwaeaborwa, O.M., Kroon, R.E., Kumar, V., Dubroca, T., Ahn, J.P., Park, J.K., Swart, H.C.: Ex-situ synthesis and optical properties of ZnO–PbS nanocomposites. *J. Phys. Chem. Solids* **70**, 1438–1442 (2009)
10. Hone, F.G., Dejene, F.B.: Six complexing agents and their effects on optical, structural, morphological and photoluminescence properties of lead sulphide thin films prepared by chemical route. *J. Lumin.* **201**, 321–328 (2018)
11. Xu, W., Shen, Y., Xie, A., Huang, F.: Synthesis and characterization of PbS nanorods in W/O microemulsion. *Russ. J. Phys. Chem. A* **83**, 2297–2301 (2009)
12. Gaiduk, A.P., Gaiduk, P.L., Larsen, A.N.: Chemical bath deposition of PbS nanocrystal: effects of substrate. *Thin Solid Films* **516**, 3791–3795 (2008)
13. Saraidarov, T., Reisfed, R., Sashchiuk, A., Lifshitz, E.: Nanocrystallites of lead sulfide in hybrid films prepared by sol-gel process. *J. Sol-Gel Sci. Technol.* **34**, 137–145 (2005)
14. Kuang, D., Xu, A., Fang, Y., Liu, H., Frommen, C., Fenske, D.: Surfactant-assisted growth of novel PbS dendritic nanostructures via facile hydrothermal process. *Adv. Mater.* **15**, 1747–1750 (2003)
15. Wang, S.F., Gu, F., Lu, M.K.: Sonochemical synthesis of hollow PbS nanospheres. *Langmuir* **22**, 398–401 (2006)
16. Dhlamini, M.S., Terblans, J.J., Ntwaeaborwa, O.M., Ngaruiya, J.M., Hillie, K.T., Botha, J.R., Swart, H.C.: Photoluminescence properties of powder and pulsed laser-deposited PbS nanoparticles in SiO₂. *J. Lumin.* **128**, 1997–2003 (2008)
17. Koao, L.F., Dejene, B.F., Swart, H.C., Motloung, S.V., Motloutse, T.E., Hlangothi, S.P.: Effect of Tb³⁺ ions on the ZnO nanoparticles synthesized by chemical bath deposition method. *Adv. Mater. Lett.* **7**, 529–535 (2016)
18. Hone, F.G., Ampong, F.K., Abza, T., Nkrumah, I., Paal, M., Nkum, R.K., Boakye, F.: The effect of deposition time on the structural, morphological and optical band gap of lead selenide thin films synthesized by chemical bath deposition method. *Mater. Lett.* **155**, 58–61 (2015)
19. Habte, A.G., Hone, F.G., Dejene, F.B.: The influence of malonic acid on the structural, morphological and optical properties of CdSe thin films prepared by chemical bath deposition method. *Inorg. Chem. Commun.* **103**, 107–112 (2019)
20. Bakshi, M.S., Thakur, P., Sachar, S., Kaur, G., Banipal, T.S., Possmayer, F., Petersen, N.O.: Aqueous phase surfactant selective shape controlled synthesis of lead sulfide nanocrystals. *J. Phys. Chem. C* **111**, 18087–18098 (2007)
21. Cao, H., Wang, G., Zhang, S., Zhang, X.: Growth and photoluminescence properties of PbS nanocubes. *Nanotechnology* **17**, 3280–3287 (2006)
22. Liu, S.Z., Xiong, S.L., Bao, K.Y., Cao, J., Qiang, Y.T.: Shape-controlled preparation of PbS with various dendritic hierarchical structures with the assistance of L-methionine. *J. Phys. Chem. C* **113**, 13002–13007 (2009)
23. Sadhu, S., Chowdhury, P.S., Patra, A.: Understanding the role of particle size on the photophysical properties of CdS:Eu³⁺ nanocrystals. *J. Lumin.* **126**, 387–392 (2007)
24. Hone, F.G., Dejene, F.B.: Synthesis and characterization of lead sulphide thin films from ethanalamine (ETA) complexing agent chemical bath. *Mater. Res. Express* **5**, 026409 (2018)

Publisher's Note Springer Nature remains neutral with regard to jurisdictional claims in published maps and institutional affiliations.

